

We are IntechOpen, the world's leading publisher of Open Access books Built by scientists, for scientists

6,900

Open access books available

186,000

International authors and editors

200M

Downloads

Our authors are among the

154

Countries delivered to

TOP 1%

most cited scientists

12.2%

Contributors from top 500 universities



WEB OF SCIENCE™

Selection of our books indexed in the Book Citation Index
in Web of Science™ Core Collection (BKCI)

Interested in publishing with us?
Contact book.department@intechopen.com

Numbers displayed above are based on latest data collected.
For more information visit www.intechopen.com



Mechanical Properties of GO Nanostructures Prepared from Freeze-Drying Method

Yanhui Ding, Hui Chen, Zheng Li, Huming Ren, Xianqiong Tang, Jiuren Yin, Yong Jiang and Ping Zhang

Additional information is available at the end of the chapter

<http://dx.doi.org/10.5772/intechopen.71515>

Abstract

Recently, 3D graphene oxide (GO) has attracted much attention due to its high specific surface area, multifunction, and facile preparation. Here, porous GO foams with extraordinary mechanical properties were prepared by using freeze-drying technique. The structure and mechanical properties of the GO foams have been characterized by X-ray diffraction, Fourier transform infrared spectroscopy, atomic force microscopy, and electronic universal testing machine. The unique structure endows the GO foams excellent elasticity, which can recover to its original shape even after compression hundreds of times. The density of GO foams has a significantly positive impact on the elastic modulus. Furthermore, the compressive strength of GO foams decreased linearly with decreasing relative humidity. A honeycomb model was constructed to investigate the effects of wall thickness, length, and included angle on the elastic modulus of GO foams. The structural evolution during the compression was revealed by finite element simulation.

Keywords: GO foams, mechanical properties, humidity sensitivity, Gibson honeycomb model, finite element simulation

1. Introduction

Recently, graphene and graphene oxide (GO) have been widely studied for various applications, such as sensors, field-effect transistors, Li-ion batteries, and polymer composites, due to their remarkable physical and chemical properties. As is well known, preparation of

graphene monolayers by chemical reduction of GO sheets is considered as an ideal method to obtain a high yield of graphene. Actually, GO is a kind of functional nanomaterials used widely, which contains large number of hydrophilic groups such as hydroxyl, carboxyl, and carbonyl on both sides of the sheets. Since graphene was reckoned as a strong contender to carbon nanotubes, GO-based materials have attracted a great deal of attention due to their wide applications in gas sensors [1], Li-storage [2, 3], catalyst supports [4], and water purification [5]. GO nanosheets can be easily prepared by chemical exfoliation of graphite in bulk quantities. Due to its good dispersity and ease of post-functionalization, the researchers not only focus on the reduction of GO to graphene but also shift to explore various chemical and physical properties caused by chemical modification and structure tuning. Theoretical and experimental studies have demonstrated that GO exhibited size-dependent properties when its size down to the nanometer scale. GO sheets with different lateral size displayed different mechanical strength.

Though we view GO as potentially powerful and widely applicable, it is very difficult to recycle GO from the dispersion. To overcome this problem, various methods such as blending GO with polymer matrix, formation of GO sponge, and chemical reduced GO gels generated by hydrothermal method have been investigated. Recently, significant progress has been made in self-assembly of GO nanosheets into microporous or mesoporous networks such as GO foams. Several methods have been employed to prepare 3D GO foams such as self-assembly [6, 7], leavening process [8], electrochemical erosion [9], electrospinning method [10, 11], hydrothermal reaction [12], solvent evaporation method [13], and freeze-drying technique [14–16]. Among them, the freeze-drying technique has been intensively studied due to its low-cost, high efficiency, and high yield. The mechanical performance of GO foam is critical to its application under harsh environments; however, most researchers focused on the functionality of GO architectures. Here, 3D GO foams were prepared by freeze drying of GO aqueous dispersion. The relationship between structure and mechanical behavior of GO foams was investigated, and the effect of RH on the mechanical properties of GO foams was also studied. Simultaneously, the structural evolution of GO under uniaxial compression was simulated by finite element method.

2. Experimental details

2.1. Preparation of GO nanosheets

We used a modified Hummers' method to produce chemical exfoliated GO nanosheets with a thickness of 2–5 nm and lateral dimensions of 1–10 μm . In a typical process, graphite powders were oxidized by reacting with a mixture of NaNO_3 and concentrated H_2SO_4 in an ice bath, then KMnO_4 was added to the dispersion slowly. After fully oxidizing, the graphite oxide was washed with dilute HCl and deionized water pH of the wash solution was near neutral. The obtained graphite oxide was dispersed in deionized water and exfoliated through ultrasonication for 0.5 h.

2.2. Preparation of GO foams

GO foams were fabricated by freeze-drying method to form GO dispersion. The concentration of GO was set at 6.8 gL^{-1} . GO suspension was frozen into an ice cube in a refrigerator (-18°C) and then freeze dried with a condenser temperature of -20°C and inside pressure less than 20 Pa.

2.3. Tests of GO foams

The morphology, structure, and mechanical properties of GO foam were investigated by X-ray diffraction (XRD; Bruker D8 Advance), Fourier transform infrared spectroscopy (FTIR; Perkin-Elmer Spectrum 10), scanning electronic microscopy (SEM; JSM-6610LV), atomic force microscopy (AFM; Veeco Multimode Nanoscope 3D), and electronic universal testing machine (UTM; Instron 5943). The diameter and height of the specimens were 10 and 5 mm, respectively.

3. Results and discussion

AFM image, XRD pattern, and FTIR spectra of as-prepared GO foam are shown in **Figure 1**. Exfoliation of graphite oxide to GO was achieved by ultrasonication of graphite oxide. The exfoliated GO nanosheets are flat with an average thickness of about 2 nm, which means that the single-layer GO sheet was obtained, as shown in **Figure 1a**. XRD pattern of GO contains an intense 001 peak at $2\theta = 10^{\circ}$ that corresponds to a d-spacing of approximately 0.8 nm. The disappearance of the native graphite peak at about 26° revealed the successful oxidation of the graphite powders. The increased interlayer spacing can weaken the van der Waals interactions between GO layers and make facile exfoliation possible. FTIR spectra of GO show that the spectral bands are corresponding to C-O stretching vibrations ($1300\text{--}1000 \text{ cm}^{-1}$), C=O stretching vibrations from carbonyl and carboxylic groups ($1720\text{--}1706 \text{ cm}^{-1}$), C=C stretching vibrations from unoxidized graphitic domains ($1450\text{--}1680 \text{ cm}^{-1}$), C-H bending vibration ($1465\text{--}1340 \text{ cm}^{-1}$), and O-H stretching vibrations (3430 cm^{-1}) [17, 18]. The presence of these functional groups on the GO surface leads to strong interaction of GO with water. In addition, the presence of the functional groups makes GO thermally unstable, as it undergoes pyrolysis at elevated temperatures.

Digital picture of a cylinder-like GO foam is presented in **Figure 2a**. The shape and size of the GO foam can be easily adjusted in the freeze-drying process. Foam-like structures with high porosity and flexibility have many important applications in actuators, catalytic supports, adsorption, and separation. The size of the foam can be easily adjusted by simply changing the initial concentration of the GO suspension. SEM image reveals that interconnected pore structure is formed where GO nanosheets traversed laterally and connected with other sheets. This honeycomb features endow GO foam extraordinary mechanical properties, which can undergo compression without collapsing.

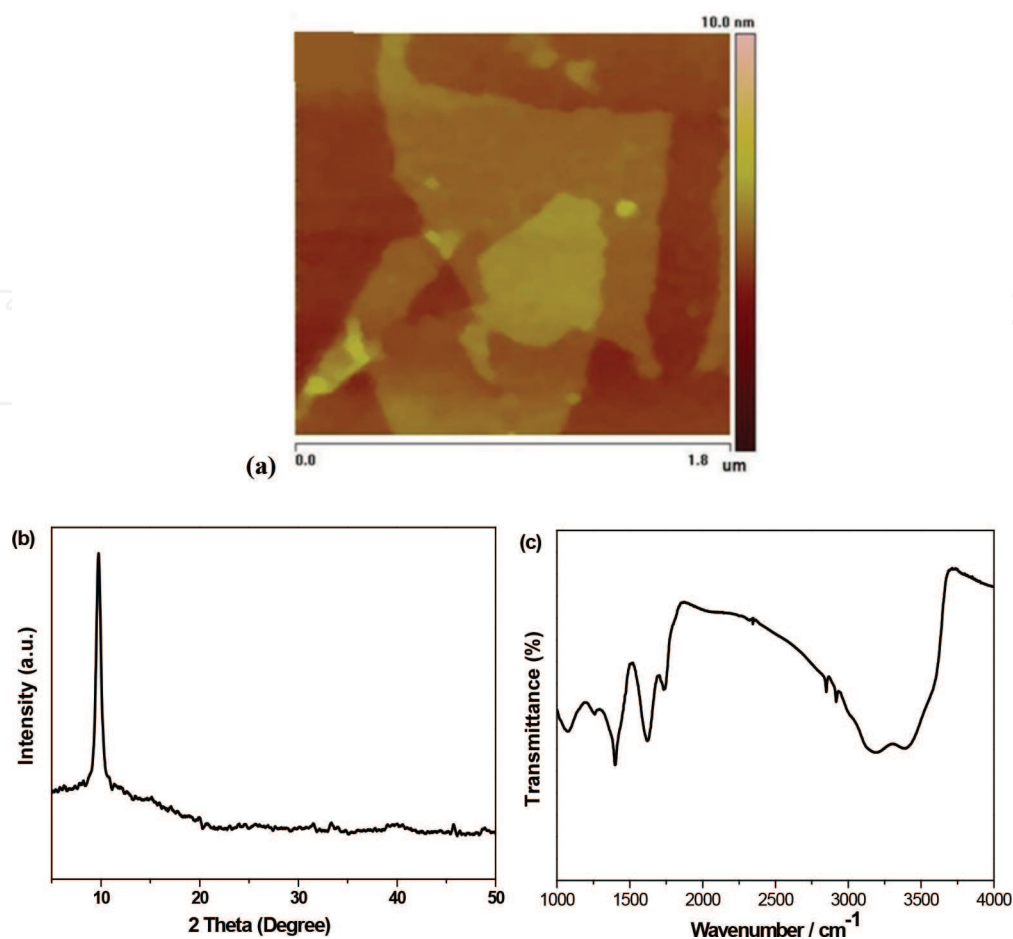


Figure 1. AFM image, XRD pattern, and FTIR spectra of as-prepared GO. (a) AFM image; (b) XRD; (c) FTIR.

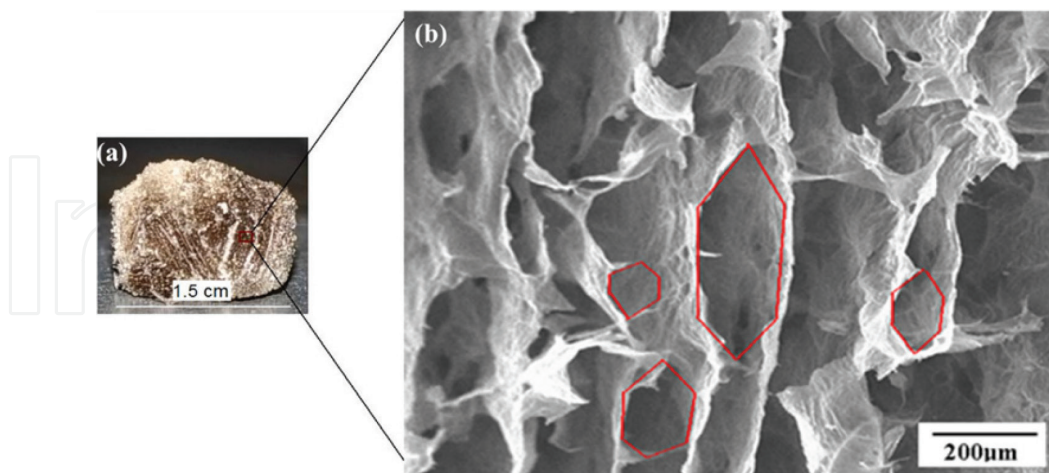


Figure 2. Microstructure of GO foams. The red line shows the honeycomb-like structure in GO foam.

GO foams were submitted to compression for 300 cycles, and each cycle involved an contact between sample and the indenter, a displacement to a prescribed value, and a retraction to the original position. The results of uniaxial compression experiments are shown in **Figure 3a**.

A compression load of 1.5 N was applied, and GO foams were pressed to 80% of the original length. After 300 cycles, the compression load was not changed, which can be ascribed to the well-ordered microstructures oriented along the compression direction. The load-displacement curves recorded during the compression cycling are shown in **Figure 3b**. All curves have a familiar form, in which displacement increases as applied load gradually increases. Once a maximum value of 1.5 N is achieved, the load decreases as the indenter is retracted. As we can see from the figure, no residual displacement is observed after the indenter was fully retracted. GO foams exhibited good elasticity, and it recovered to its original height even after 300 cycles.

The humidity sensitivity of the GO foam was characterized. As depicted in **Figure 4**, the maximum load compressed GO foam to its 80% of the original length is reduced with the increasing of RH. Surface properties of GO sheets were affected greatly by the RH due to its hydrophilicity, which caused a change in the mechanical behavior of GO foams.

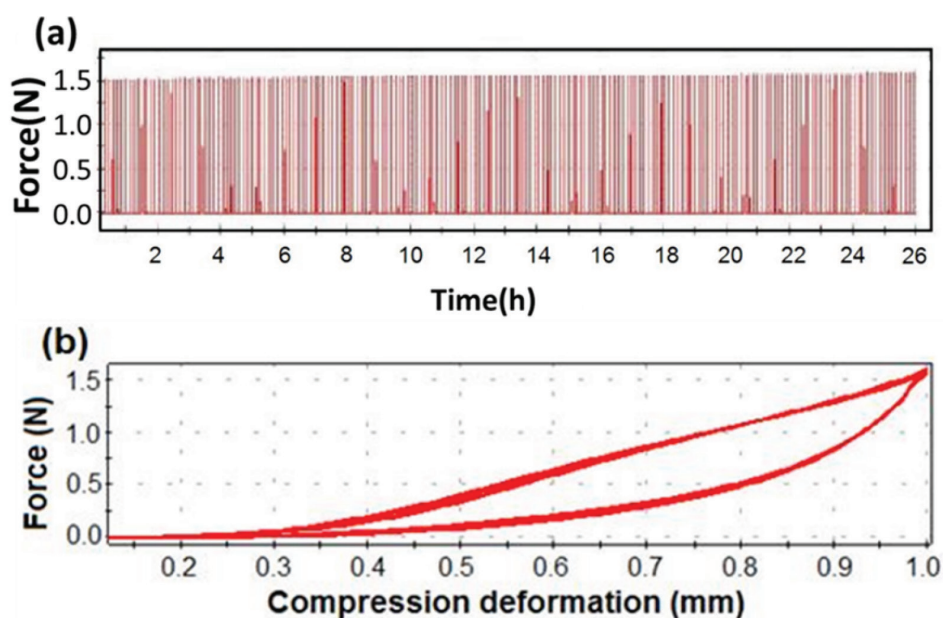


Figure 3. Uniaxial compression data of GO foams. (a) Uniaxial compression test. (b) Compression cycling.

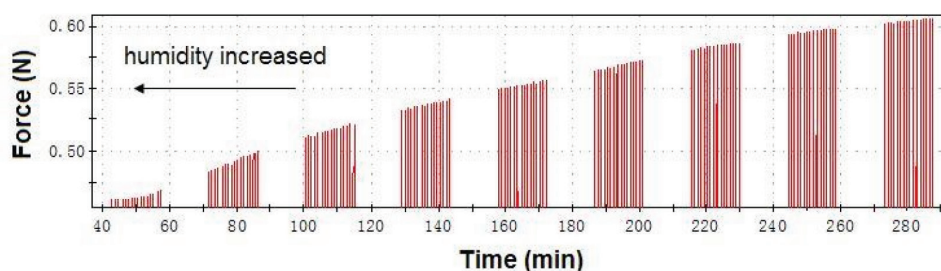


Figure 4. Load-displacement curves at different ambient humidity.

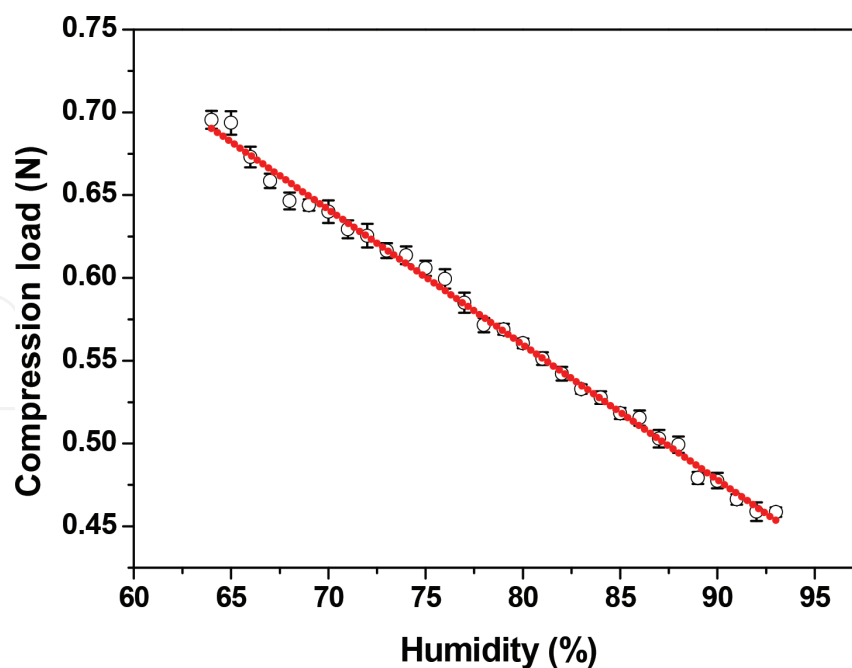


Figure 5. Relationship between the RH and mechanical properties of GO foams.

The relationship between the RH and mechanical properties of GO foams was shown in **Figure 5**. It is surprise that a linear relationship is observed between the maximum compression load and RH. GO foam exhibited very high sensitivity and good linearity with the RH in the range of 65–93%. Here, we give some discussions about the humidity sensing mechanism of the GO nanostructures. We believed that the large decrease in mechanical properties of GO foams was related to the adsorption of water molecules. As porous structure materials, GO foams have higher specific surface areas to absorb moisture easily. Thus, striking interaction between GO sheets was released due to the lubrication of water molecules. It may be the main reason for the decay of mechanical properties.

The pore size and porosity of GO foams were easily adjusted by changing the concentration of GO dispersions in the freeze-drying process. The effects of density and strain rate on the mechanical properties of GO foams are presented in **Figure 6**. The elastic modulus of GO foams with a density of 5.25, 10.93, and 15.45 mg cm⁻³ are 0.0635, 0.1715, and 0.3822 MPa, respectively. As expected, the elastic modulus was significantly affected by the density of the GO foam. GO foam shows a high resistance against the compression with increasing density. The yield stress displayed an increase as the strain rate increased due to the strain rate-dependent behavior of GO foams.

A honeycomb structure was constructed for the calculation of elastic modulus of GO foam. Two hypotheses were proposed: (1) GO foam suffers small deformation under uniaxial compression. (2) Honeycomb structure is remained during the compression. Then, the elastic modulus E and Poisson's ratio ν could be expressed as:

$$\left. \begin{aligned} E &= \frac{E_s \left(\frac{t}{l}\right)^3 \left(\cos \theta + \frac{t}{l}\right)}{\left[\left(\frac{h}{l} + \sin \theta\right) \sin^2 \theta\right] \cdot \left[1 + (2.4 + 1.5 v_s + \cot^2 \theta) \left(\frac{t}{l}\right)^2\right]} \\ v_{12} &= \frac{\left(\cos \theta + \frac{t}{l}\right) \cos \theta \cdot \left[1 + (1.4 + 1.5 v_s) \left(\frac{t}{l}\right)^2\right]}{\left[\left(\frac{h}{l} + \sin \theta\right) \sin \theta\right] \cdot \left[1 + (2.4 + 1.5 v_s + \cot^2 \theta) \left(\frac{t}{l}\right)^2\right]} \end{aligned} \right\} \quad (1)$$

Where t , l , and θ are the wall thickness, length, and included angle, respectively. The effects of wall thickness, length, and included angle on the mechanical properties of GO foams are shown in **Figure 7**. With an increase of h/l , the elastic modulus of GO foams decreased. However, the elastic modulus decreased with decreasing t/l . Additionally, the elastic modulus decreased with an increase in structural parameter θ .

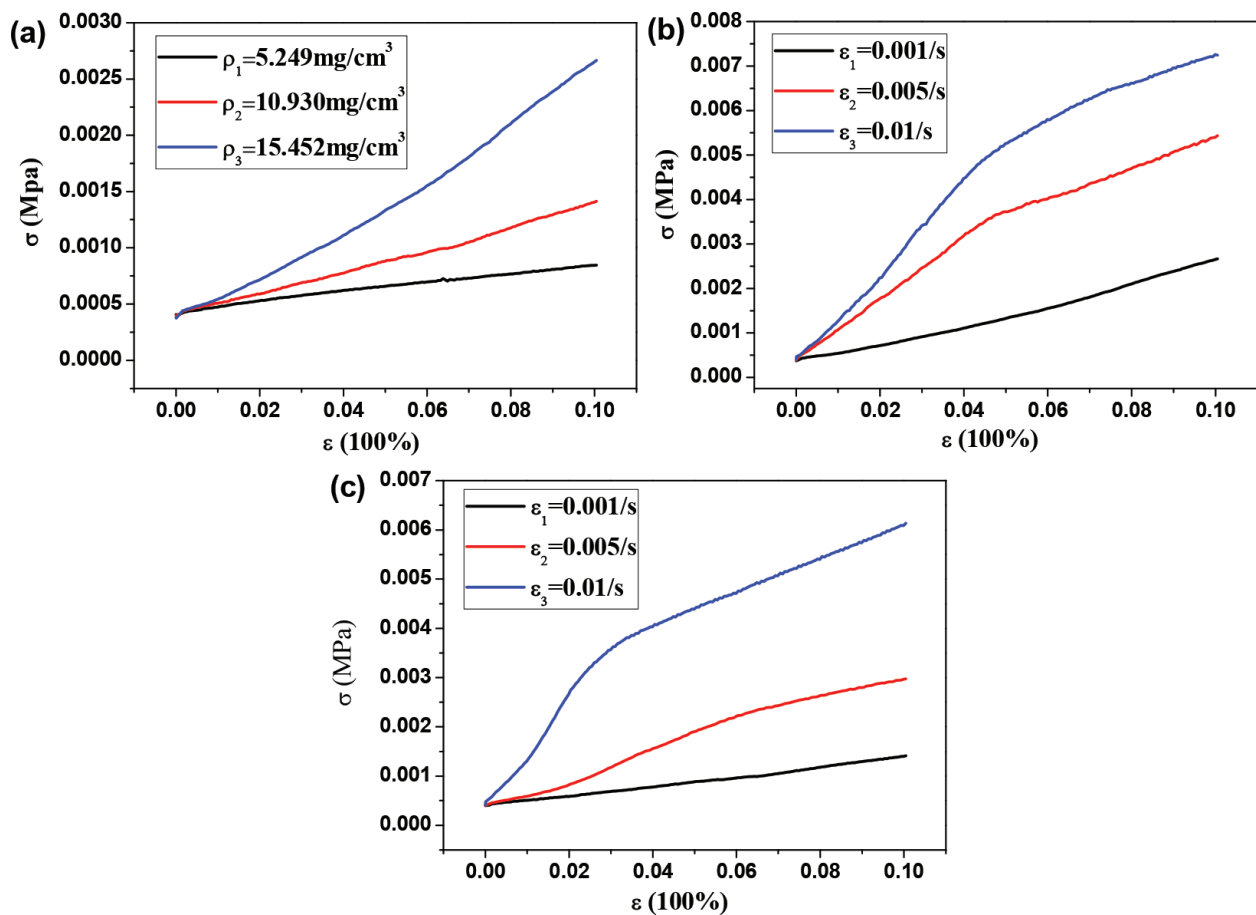


Figure 6. Effects of density and strain rate on the stress-strain behaviors of GO foams. (a) Loading rate 1 mm min^{-1} ; (b) density 15.45 mg cm^{-3} ; (c) density 10.93 mg cm^{-3} .

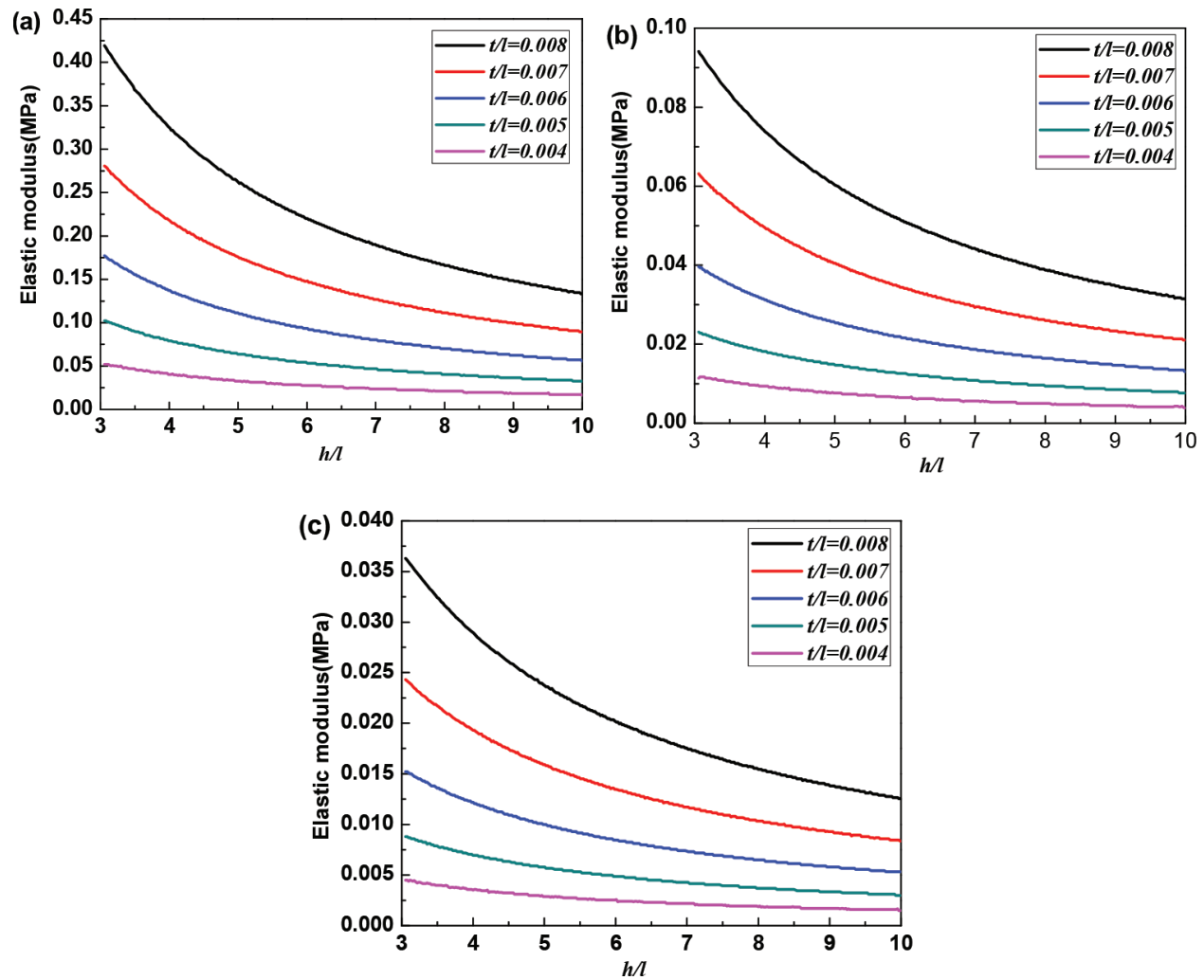


Figure 7. Effects of wall thickness (t), length (l), and included angle (θ) on the elastic modulus of GO foams. (a) $\theta = 15^\circ$; (b) $\theta = 30^\circ$; and (c) $\theta = 45^\circ$.

The change of honeycomb-like GO foams before and after compression was simulated by FE method as shown in **Figure 8**. The FE model was created in Commercial software package (ANSYS 15.0). The bottom was fixed and the compression force was applied on the top of the model. The honeycomb structure can be described as a typical linear elastic material according to the experimental data. Then, the effect of cell size on the mechanical properties of honeycomb structure was calculated by FE method. The compressive stress of GO foams under small deformation can be released by the interconnected GO nanosheets. The strain was mainly concentrated at the middle of the long side when honeycomb structure undergone large deformation as shown in the strain nephogram. Buckling is the type of failure that has been observed in GO foam after compression. From the SEM image, the FE simulation has been proven to be effective in this case. The deformation of the honeycomb-like structure is mainly observed at the long side wall of the cell, which is consistent with the simulation results.

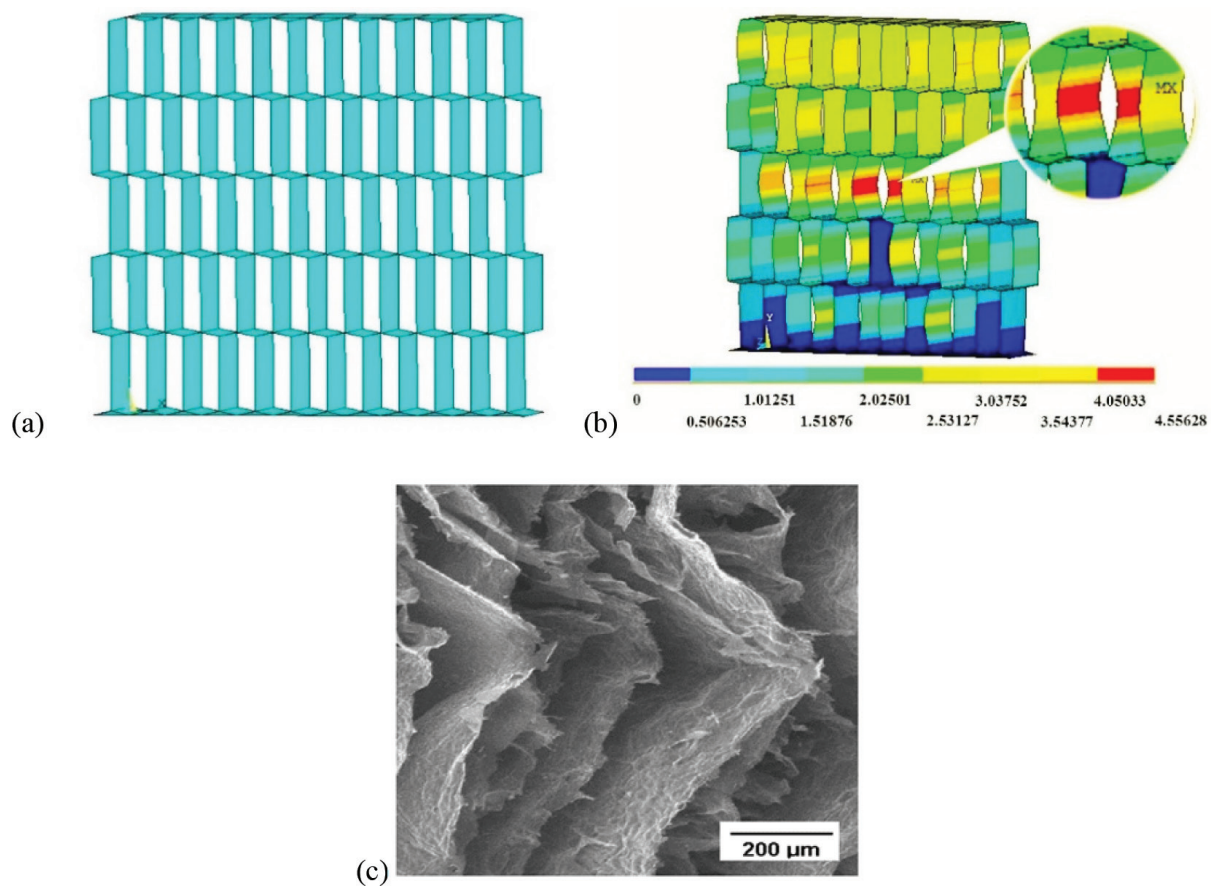


Figure 8. FE simulation and SEM image of honeycomb-like GO foams before and after compression. The insert in **Figure 8b** represents the strain concentrates on the middle of the long side.

4. Conclusions

Honeycomb-like structured GO foams were prepared by freeze-drying method. The GO network structure endows GO foam extraordinary mechanical properties. GO foams can recover to its original height even after 300 compression cycles. GO foams exhibits a linear relationship between the maximum compression load and RH. SEM characterization reveals that the deformation of the honeycomb-like structure under compression is mainly observed at the long side wall of the cell, which is consistent with the FE simulation results.

Acknowledgements

The financial support from the National Natural Science Foundation of China (No. 21376199 and 51,002,128) and Scientific Research Foundation of Hunan Provincial Education Department (No. 17A205) is greatly acknowledged.

Author details

Yanhuai Ding, Hui Chen, Zheng Li, Huming Ren, Xianqiong Tang, Jiuren Yin, Yong Jiang and Ping Zhang*

*Address all correspondence to: zhangp@xtu.edu.cn

Institute of Rheological Mechanics, Xiangtan University, Hunan, China

References

- [1] Ming R, Ding Y, Chang F, He X, Feng J, Wang C, Zhang P. Humidity-dependant compression properties of graphene oxide foams prepared by freeze-drying technique. *IET Micro & Nano Letters*. 2013;**8**:66
- [2] Compton OC, Nguyen ST. Graphene oxide, highly reduced graphene oxide, and graphene: Versatile building blocks for carbon-based materials. *Small*. 2010;**6**:711
- [3] Vickery JL, Patil AJ, Mann S. Fabrication of graphene-polymer nanocomposites with higher-order three-dimensional architectures. *Advanced Materials*. 2009;**21**:2180
- [4] Long Y, Zhang C, Wang X, Gao J, Wang W, Liu Y. Oxidation of SO₂ to SO₃ catalyzed by graphene oxide foams. *Journal of Materials Chemistry*. 2011;**21**:13934
- [5] He Y, Liu Y, Wu T, Ma J, Wang X, Gong Q, Kong W, Xing F, Liu Y, Gao J. An environmentally friendly method for the fabrication of reduced graphene oxide foam with a super oil absorption capacity. *Journal of Hazardous Materials*. 2013;**260**:796
- [6] Huang X, Qian K, Yang J, Zhang J, Li L, Yu C, Zhao D. Functional nanoporous graphene foams with controlled pore sizes. *Advanced Materials*. 2012;**24**:4419
- [7] Chen W, Li S, Chen C, Yan L. Self-assembly and embedding of nanoparticles by in situ reduced graphene for preparation of a 3D graphene/nanoparticle aerogel. *Advanced Materials*. 2011;**23**:5679
- [8] Niu Z, Chen J, Hng HH, Ma J, Chen X. A leavening strategy to prepare reduced graphene oxide foams. *Advanced Materials*. 2012;**24**:4144
- [9] Favaro M, Agnoli S, Cattelan M, Moretto A, Durante C, Leonardi S, Kunze-Liebhäuser J, Schneider O, Gennaro A, Granozzi G. Shaping graphene oxide by electrochemistry: From foams to self-assembled molecular materials. *Carbon*. 2014;**77**:405
- [10] Chen Y, Lu Z, Zhou L, Mai Y-W, Huang H. Triple-coaxial electrospun amorphous carbon nanotubes with hollow graphitic carbon nanospheres for high-performance Li ion batteries. *Energy & Environmental Science*. 2012;**5**:7898
- [11] Chen Y, Li X, Zhou X, Yao H, Huang H, Mai Y-W, Zhou L. Hollow-tunneled graphitic carbon nanofibers through Ni-diffusion-induced graphitization as high-performance anode materials. *Energy & Environmental Science*. 2014;**7**:2689

- [12] Xu Y, Sheng K, Li C, Shi G. Self-assembled graphene hydrogel via a one-step hydrothermal process. *ACS Nano*. 2010;**4**:4324
- [13] Ding Y-H, Zhang P, Ren H-M, Zhuo Q, Yang Z-M, Jiang Y. Preparation of graphene/TiO₂ anode materials for lithium-ion batteries by a novel precipitation method. *Materials Research Bulletin*. 2011;**46**:2403
- [14] Ye S, Feng J, Wu P. Highly elastic graphene oxide-epoxy composite aerogels via simple freeze-drying and subsequent routine curing. *Journal of Materials Chemistry A*. 2013;**1**:3495
- [15] Mi X, Huang G, Xie W, Wang W, Liu Y, Gao JP. Preparation of graphene oxide aerogel and its adsorption for Cu²⁺ ions. *Journal of Carbon*. 2012;**50**:4856
- [16] Mohandes F, Salavati-Niasari M. Freeze-drying synthesis, characterization and in vitro bioactivity of chitosan/graphene oxide/hydroxyapatite nanocomposite. *RSC Advances*. 2014;**4**:25993
- [17] Guo H-L, Wang X-F, Qian Q-Y, Wang F-B, Xia X-H. A green approach to the synthesis of graphene nanosheets. *ACS Nano*. 2009;**3**:2653-2659
- [18] Cote LJ, Cruz-Silva R, Huang J. Flash reduction and patterning of graphite oxide and its polymer composite. *Journal of the American Chemical Society*. 2009;**131**:11027-11032

